ACS OMEGA

Open Access

This article is licensed under CC-BY-NC-ND 4.0

http://pubs.acs.org/journal/acsodf

Article

Design and Synthesis of Pyrimidine Amine Containing Isothiazole Coumarins for Fungal Control

Kun Li, Mengyuan Li, Haolin Zhong, Liangfu Tang, You Lv,* and Zhijin Fan*

Cite This: *ACS Omega* 2023, 8, 37471−37481

Read Online

ACCESS | Metrics & More | Article Recommendations | Supporting Information

ABSTRACT: Developing new fungicides is always crucial to protecting crops. A series of 4-(3,4-dichloroisothiazol-5-yl)-7-(2-((5-(5-pyrimidin-4-yl)amino)ethoxy)-8-methyl) coumarin derivatives were designed and synthesized by Williamson ether condensation and substitution reactions. Structure determinations were clarified by ^{1}H NMR, ^{13}C NMR, and HRMS, and compound **4h** crystallized by the fusion method for further structural confirmation. The in vitro bioassay results showed that the target compounds displayed good fungicidal activity against *Alternaria solani*, *Botrytis cinerea*, *Cercospora arachidicola*, *Fusarium graminearum*, *Physalospora piricola*, *Rhizoctonia solani*, and *Sclerotinia sclerotiorum*. Among them, compounds **4b** and **4d** showed higher inhibitory activity against *R. solani*, with EC_{50} values of 11.3 and 13.7 μg/mL, respectively, and they were more active than the positive control diflumetorim with an EC_{50} value of 19.8 μg/mL. Molecular docking suggested that compound **4b** and diflumetorim may have similar interactions with complex I NADH oxidoreductase. Density functional theory calculation and pesticide-likeness analysis studies gave a rational explanation of their fungicidal activity. These results indicated that compounds **4b** and **4d** deserved further optimization according to the principle of pesticide-likeness.

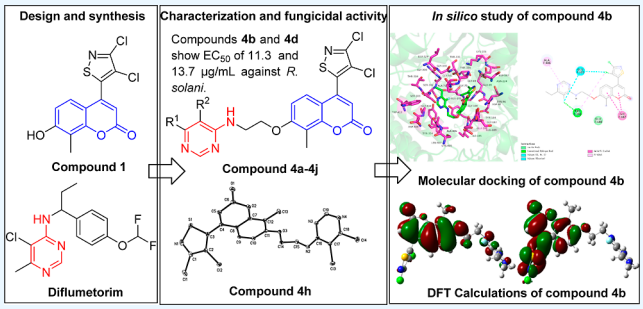

INTRODUCTION

Plant pathogenic fungi are one of the most common sources of plant diseases.[1,2] They are able to invade plant tissues and cause a range of diseases that can have a serious impact on plant growth and development.[3,4] To prevent the damage caused by plant pathogenic fungi, agricultural fungicides are often used to reduce the impact of plant diseases.[5] However, with the long-term use of fungicides, the problem of fungicide resistance has become more prevalent and serious and has become a major challenge for chemical control.[6] Expanding the diversity of lead structures to create novel fungicides is one of the most commonly used methods to address the issue of fungicide resistance.

The strategy for the development of new pesticides is mainly based on targets and leads.[7,8] The discovery of new targets is relatively difficult; thus, the discovery of new leads becomes an effective measure. Natural products are important sources of pesticide lead.[9,10] Pyrimidine amines are a class of natural alkaloids with numerous physiological and agrochemical activities.[11] According to the Fungicide Resistance Action Committee (FRAC), the fungicidal mode of action of pyrimidine-based fungicides is inhibiting NADH oxidoreductase of complex I.[12,13] So far, those that have been reported to act on complex I NADH oxidoreductase and classified by the FRAC are diflumetorim, tolfenpyrad, and fenazaquin (Figure 1).

Coumarins are benzopyrone heterocyclic compounds that are naturally found in various herbs and plants.[14,15] Also, coumarins have good anti-inflammatory,[16] antibacterial,[17] anticancer,[18] antioxidant,[19] anti-HIV,[20] and antiviral[21] activity. The presence and location of phenolic hydroxyl groups on the coumarin backbone were found to be very important for activity.[22] 7-Hydroxycoumarin is one of the coumarins with antifungal,[23] anticancer,[24] and anti-inflammatory activity[25] and can be used as pharmaceutical intermediates.

Previously, by combining the 3,4-dichloroisothiazole structure with 7-hydroxycoumarin, we discovered the highly active isothiazole coumarin derivatives 4-(3,4-dichloroisothiazol-5-yl)-7-hydroxy-8-methyl-2*H*-coumarin (**1**), which exhibited high efficacy against *Rhizoctonia solani* and *Pseudoperonospora cubensis*.[26] In this work, using compound **1** as the lead compound, the introduction of the active substructural unit of naturally based pyrimidine amine into the target molecules, and the linkage of coumarins to pyrimidine structures using bromoethylamine as a bridge chain, 10 coumarin pyrimidine amine derivatives were designed, synthesized, and their

Received: August 4, 2023
Accepted: September 13, 2023
Published: September 28, 2023

ACS Publications

© 2023 The Authors. Published by American Chemical Society

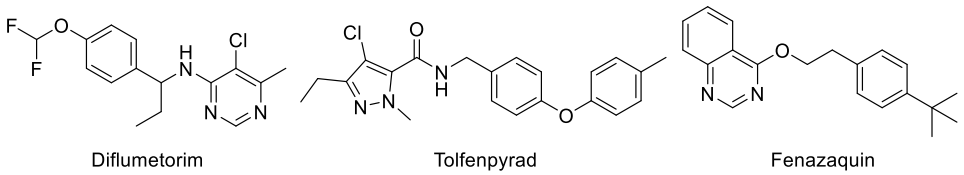

Figure 1. Reported fungicides acting on complex I NADH oxidoreductase.

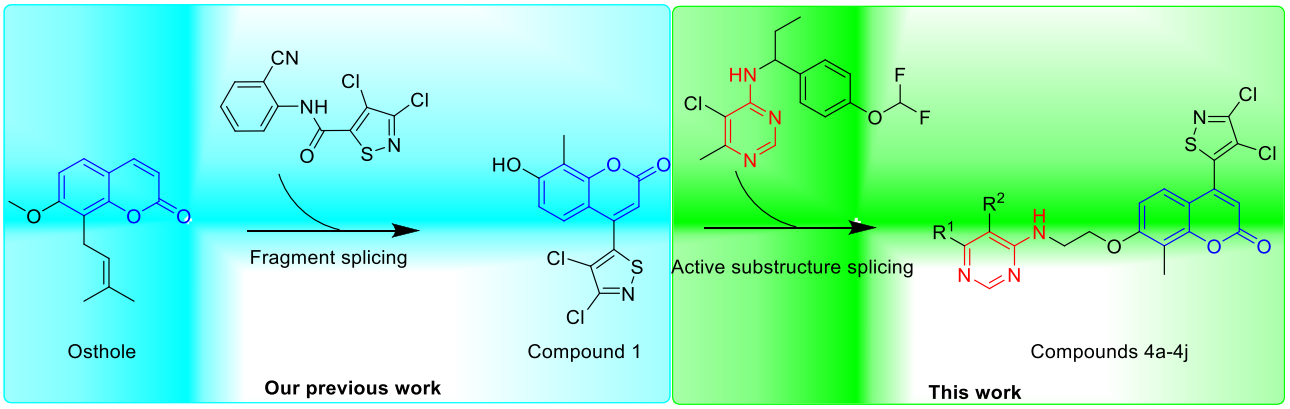

Figure 2. Design of the target compound.

Scheme 1. Synthetic Route of Target Compounds 4a−4j[a]

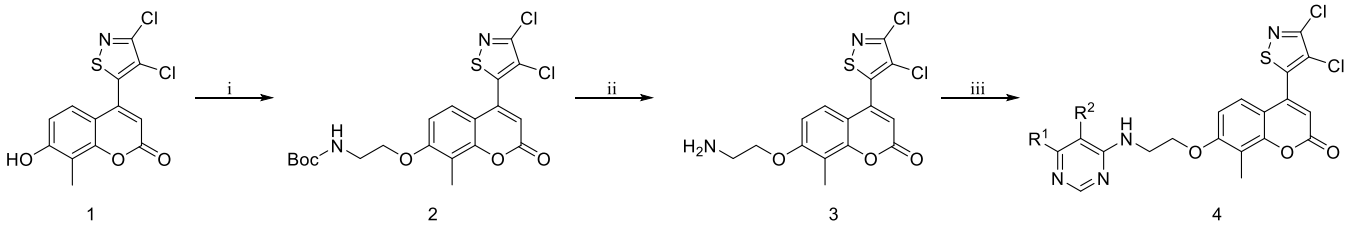

4a: R^1=CH_3,R^2=Br; 4b: R^1=CH_3CH_2,R^2=F; 4c: R^1=Cl,R^2=CN; 4d: R^1=Cyclopropyl,R^2=F; 4e: R^1=Cyclopropyl,R^2=Cl;
4f: R^1=Cl,R^2=CH_3; 4g: R^1=CHF_2,R^2=Cl; 4h: R^1=Cl,R^2=Cl; 4i: R^1=CH_3CH_2,R^2=Cl; 4j: R^1=CH_3,R^2=Cl;

[a]Reagents and conditions: (i) *tert*-butyl-2-bromoethyl carbamate, K_2CO_3, DMF, 80 °C, overnight. (ii) CF_3COOH, DCM, r.t., overnight. (iii) Substituted chloro-pyrimidines, K_2CO_3, DMF, 80 °C, 7−8 h.

antifungal activity was evaluated (Figure 2). The synthetic route of the target compounds is shown in Scheme 1.

MATERIALS AND METHODS

X-4 digital type melting point tester (Gongyi, China); Bruker AV400 MHz (Wisconsin, United States of America, TMS as the internal standard, $CDCl_3$ or DMSO-d_6 as solvent); Agilent 6520 Q-TOF LC/MS high-resolution mass spectrometer (Agilent Technologies Inc., Ltd.); column chromatography silica gel (100−200 mesh); and thin-layer chromatography silica plate (Yantai Xinnuo Chemical Co.); all reagents and solvents were obtained from commercial sources and used without further purification; the positive control osthole was purchased from Shanghai Macklin Inc.; and the positive control diflumetorim was prepared by our group.

General Procedures for Preparation of Compound 2. Compound **1** was synthesized according to the reported method.[26] Compound **1** (1.0 mmol) and potassium carbonate (3.5 mmol) were added to a 50 mL flask, and then 10 mL of DMF was added. After the reaction mixture was stirred at 60 °C for 5 min, *tert*-butyl (2-bromoethyl) carbamate (3.0 mmol) was added, then the temperature was raised to 80 °C, and the reaction was allowed to proceed overnight. After the reaction mixture was cooled to room temperature, water (15 mL) was added. The resulting mixture was extracted with ethyl acetate (3 × 20 mL), and the organic phases were combined. The combined organic solution was washed sequentially with water (3 × 10 mL) and brine (10 mL). The resultant organic layer was dried in anhydrous Na_2SO_4. The solvent was evaporated under reduced pressure, and the residue was purified by column chromatography on a silica gel (100−200 mesh) with a mixture of ethyl acetate/petroleum ether (60−90 °C fraction) (1:20−1:10, v/v) to give compound **2**.

Analytical Data for Compound 2. White solid; yield: 90%; mp 146−147 °C; ^{1}H NMR (400 MHz, DMSO-d_6): δ 7.23 (d, J = 8.8 Hz, 1H), 7.06 (t, J = 5.7 Hz, 1H), 7.02 (d, J = 9.0 Hz, 1H), 6.54 (s, 1H), 4.08 (t, J = 5.4 Hz, 2H), 3.38−3.34 (m, 2H), 2.23 (s, 3H), 1.37 (s, 9H); ^{13}C NMR (100 MHz, DMSO-d_6): δ 159.89, 159.01, 155.67, 155.01, 152.18, 147.15, 142.95, 124.90, 121.18, 114.57, 113.37, 110.36, 108.65, 77.73, 67.73, 28.16, 7.95 (one carbon atom overlaps with DMSO-d_6); HRMS (m/z): calcd for $C_{20}H_{20}Cl_2N_2NaO_5S$ $(M + Na)^+$, 493.0368; found, 493.0360.

General Procedures for Preparation of Compound 3. Compound **2** (10.0 mmol), trifluoroacetic acid (10 mL), and

https://doi.org/10.1021/acsomega.3c05734
ACS Omega 2023, 8, 37471−37481

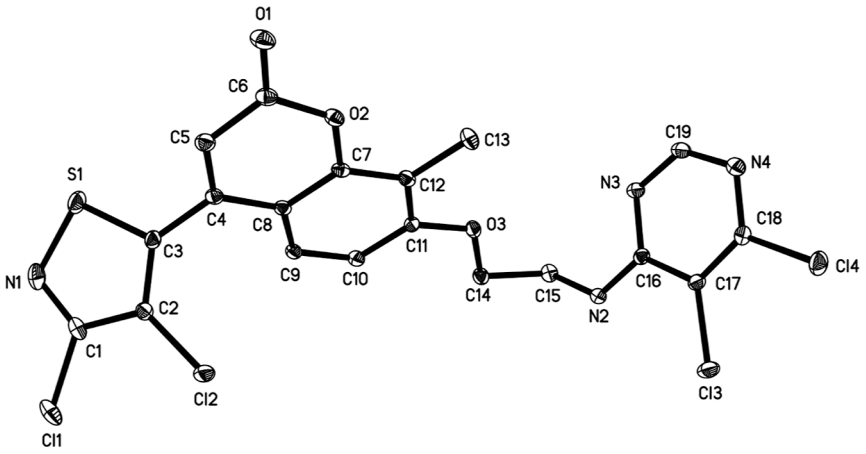

Figure 3. X-ray crystal structure of compound **4h** (CCDC: 2286889).

Table 1. Crystal Data and Structure Refinement for Compound 4h

compound	**4h**
empirical formula	$C_{19}H_{12}Cl_4N_4O_3S$
formula weight	518.19
temperature/K	113.15
crystal system	monoclinic
space group	$P2_1/n$
a/Å	10.4726(2)
b/Å	13.4198(2)
c/Å	14.4509(3)
α/deg	90
β/deg	89.987(2)
γ/deg	90
volume/Å^3	2030.93(6)
Z	4
ρ_{calc} g/cm^3	1.695
μ/mm^{-1}	0.718
F (000)	1048.0
crystal size/mm^3	0.26 × 0.23 × 0.17
radiation	Mo Kα (λ = 0.71073)
2Θ range for data collection/deg	4.142 to 69.472
index ranges	$-16 \le h \le 16$, $-20 \le k \le 20$, $-22 \le l \le 20$
reflections collected	31,796
independent reflections	7552 [R_{int} = 0.0482, R_{sigma} = 0.0460]
data/restraints/parameters	7552/0/281
goodness-of-fit on F^2	1.021
final R indexes [$I \ge 2\sigma$ (I)]	R_1 = 0.0508, wR_2 = 0.1113
final R indexes [all data]	R_1 = 0.0743, wR_2 = 0.1232
largest diff. peak/hole/e Å^{-3}	0.57/−0.33

dichloromethane (20 mL) were added to a 100 mL flask and allowed to react overnight at room temperature. After water (20 mL) was added, the reaction mixture was extracted with ethyl acetate (3 × 20 mL), and the organic phases were combined, dried over anhydrous Na_2SO_4, and filtered. The filtrate was concentrated and compound **3** was obtained.

Analytical Data for Compound 3. Yellow solid; yield: 92%; mp 121−123 °C; ^{1}H NMR (400 MHz, chloroform-d): δ 7.13 (d, J = 8.8 Hz, 1H), 6.82 (d, J = 8.9 Hz, 1H), 6.31 (s, 1H), 4.10 (t, J = 5.2 Hz, 2H), 3.16 (t, J = 5.1 Hz, 2H), 2.36 (s, 3H), 1.53 (s, 2H) (NH_2(br, 2H) overlap with H_2O). ^{13}C NMR (100 MHz, chloroform-d): δ 160.68, 159.76, 154.48, 153.03, 149.39, 142.92, 124.39, 122.35, 115.12, 114.72, 110.49, 108.15, 71.16, 41.40, 8.32. HRMS (m/z): calcd for $C_{15}H_{13}Cl_2N_2O_3S$ (M + H)$^+$, 371.0018; found, 371.0016.

General Procedures for Preparation of Target Compounds 4a−4j. Compound **3** (0.61 mmol), substituted chloropyrimidines (0.58 mmol), and potassium carbonate (1.74 mmol) were added to a 50 mL flask, followed by 10 mL of DMF, and the reaction mixture was stirred at 60 °C for 7−8 h. After the reaction was completed, the reaction mixture was cooled to room temperature, and water (20 mL) was added. The resulting mixture was extracted with ethyl acetate (3 × 20 mL), and the organic phases were combined. The organic phase was washed sequentially with water (3 × 10 mL) and brine (10 mL). The resultant organic layer was dried over anhydrous Na_2SO_4. The solvent was evaporated under reduced pressure. The residue was purified by column chromatography on a silica gel (100−200 mesh) with a mixture of ethyl acetate/petroleum ether (60−90 °C fraction) (1:5−1:2, v/v) to give compounds **4**.

*Analytical Data for Compound **4a**.* 7-(2-((5-Bromo-6-methylpyrimidin-4-yl)amino)ethoxy)-4-(3,4-dichloroisothiazol-5-yl)-8-methyl-2*H*-chromen-2-one, white solid; yield: 33%; mp 194−195 °C; ^{1}H NMR (400 MHz, chloroform-d): δ 8.36 (s, 1H), 7.12 (d, J = 8.8 Hz, 1H), 6.83 (d, J = 8.9 Hz, 1H), 6.31 (s, 1H), 5.90 (t, J = 5.4 Hz, 1H), 4.27 (t, J = 5.3 Hz, 2H), 3.99 (q, J = 5.4 Hz, 2H), 2.48 (s, 3H), 2.36 (s, 3H). ^{13}C NMR (100 MHz, chloroform-d): δ 163.02, 160.23, 159.58, 158.30, 155.71, 154.37, 153.02, 149.39, 142.85, 124.46, 122.35, 115.22, 114.97, 110.76, 108.19, 104.97, 67.16, 40.60, 24.44, 8.39. HRMS (ESI) m/z: calcd for $C_{20}H_{16}BrCl_2N_4O_3S^+$ (M + H)$^+$, 540.9503; found, 540.9499.

*Analytical Data for Compound **4b**.* 4-(3,4-Dichloroisothiazol-5-yl)-7-(2-((6-ethyl-5-fluoropyrimidin-4-yl)amino)-ethoxy)-8-methyl-2*H*-chromen-2-one, white solid; yield: 32%; mp 167−168 °C; ^{1}H NMR (400 MHz, chloroform-d): δ 8.32 (s, 1H), 7.12 (d, J = 8.8 Hz, 1H), 6.84 (d, J = 8.9 Hz, 1H), 6.31 (s, 1H), 5.43 (s, 1H), 4.27 (t, J = 5.2 Hz, 2H), 4.00 (q, J = 5.4 Hz, 2H), 2.71 (qd, J = 7.6, 2.1 Hz, 2H), 2.34 (s, 3H), 1.25 (t, J = 7.6 Hz, 3H). ^{13}C NMR (100 MHz, chloroform-d): δ 160.24, 159.66, 154.36, 153.12, 153.02, 153.00 (d, J = 10.9 Hz), 151.80 (d, J = 10.9 Hz), 149.42, 143.67 (d, J = 254.7 Hz), 142.89, 124.48, 122.37, 115.17, 114.96, 110.73, 108.15, 67.35, 39.88, 23.62, 12.09 (d, J = 1.1 Hz), 8.37. ^{19}F NMR (376 MHz, chloroform-d): δ −158.20. HRMS (ESI) m/z: calcd for $C_{21}H_{18}Cl_2FN_4O_3S^+$ (M + H)$^+$, 495.0460; found, 495.0452.

*Analytical Data for Compound **4c**.* 4-Chloro-6-((2-((4-(3,4-dichloroisothiazol-5-yl)-8-methyl-2-oxo-2*H*-chromen-7-

https://doi.org/10.1021/acsomega.3c05734
ACS Omega 2023, 8, 37471−37481

yl)oxy)ethyl)amino)pyrimidine-5-carbonitrile, white solid; yield: 21%; mp 211−213 °C; ^{1}H NMR (400 MHz, DMSO-d_6): δ 8.65 (t, J = 5.0 Hz, 1H), 8.53 (s, 1H), 7.25 (d, J = 8.8 Hz, 1H), 7.07 (d, J = 8.9 Hz, 1H), 6.57 (s, 1H), 4.30 (t, J = 5.4 Hz, 2H), 3.89 (d, J = 5.4 Hz, 2H), 2.18 (s, 3H). ^{13}C NMR (100 MHz, DMSO-d_6): δ 162.67, 162.09, 160.20, 160.16, 159.48, 155.52, 152.68, 147.65, 143.44, 125.45, 121.69, 115.23, 113.89, 113.69, 111.01, 109.28, 89.93, 66.93, 40.82, 8.42. HRMS (ESI) m/z: calcd for $C_{20}H_{13}Cl_3N_5O_3S^+$ (M + H)$^+$, 507.9804; found, 507.9796.

Analytical Data for Compound ***4d***. 7-(2-((6-Cyclopropyl-5-fluoropyrimidin-4-yl)amino)ethoxy)-4-(3,4-dichloroisothiazol-5-yl)-8-methyl-2*H*-chromen-2-one, pale yellow solid; yield: 42%; mp 177−179 °C; ^{1}H NMR (400 MHz, DMSO-d_6): δ 8.11 (d, J = 1.9 Hz, 1H), 7.67 (t, J = 5.3 Hz, 1H), 7.24 (d, J = 8.9 Hz, 1H), 7.07 (d, J = 8.9 Hz, 1H), 6.56 (s, 1H), 4.27 (t, J = 5.7 Hz, 2H), 3.80 (q, J = 5.6 Hz, 2H), 2.18 (s, 3H), 2.17−2.13 (m, 1H), 1.00−0.93 (m, 4H). ^{13}C NMR (100 MHz, DMSO-d_6): δ 160.37, 159.52, 155.55, 153.48 (d, J = 9.8 Hz), 152.69, 151.66 (d, J = 11.0 Hz), 151.43 (d, J = 9.4 Hz), 147.64, 144.02 (d, J = 254.3 Hz), 143.47, 125.44, 121.69, 115.14, 113.87, 110.94, 109.29, 67.48, 40.63, 9.53, 8.99, 8.40. ^{19}F NMR (376 MHz, DMSO-d_6): δ −161.09. HRMS (ESI): calcd for $C_{22}H_{18}Cl_2FN_4O_3S^+$ (M + H)$^+$, 507.0460; found, 507.0465.

Analytical Data for Compound ***4e***. 7-(2-((5-Chloro-6-cyclopropylpyrimidin-4-yl)amino)ethoxy)-4-(3,4-dichloroisothiazol-5-yl)-8-methyl-2*H*-chromen-2-one, white solid; yield: 87%; mp 193−194 °C; ^{1}H NMR (400 MHz, DMSO-d_6): δ 8.24 (s, 1H), 7.45 (t, J = 5.6 Hz, 1H), 7.24 (d, J = 8.8 Hz, 1H), 7.08 (d, J = 9.0 Hz, 1H), 6.56 (s, 1H), 4.28 (t, J = 5.8 Hz, 2H), 3.83 (q, J = 5.6 Hz, 2H), 2.36−2.27 (m, 1H), 2.18 (s, 3H), 1.03−0.97 (m, 4H). ^{13}C NMR (100 MHz, DMSO-d_6): δ 163.61, 160.35, 159.51, 157.72, 155.59, 155.53, 152.68, 147.65, 143.46, 125.42, 121.69, 115.13, 113.86, 111.54, 110.95, 109.34, 67.25, 40.63, 13.28, 10.07, 8.40. HRMS (ESI): calcd for $C_{22}H_{18}Cl_3N_4O_3S^+$ (M + H)$^+$, 523.0165; found, 523.0163.

Analytical Data for Compound ***4f***. 7-(2-((6-Chloro-5-methylpyrimidin-4-yl)amino)ethoxy)-4-(3,4-dichloroisothiazol-5-yl)-8-methyl-2*H*-chromen-2-one, pale yellow solid; yield: 77%; mp 212−214 °C; ^{1}H NMR (400 MHz, DMSO-d_6): δ 8.19 (s, 1H), 7.43 (t, J = 5.3 Hz, 1H), 7.24 (d, J = 8.8 Hz, 1H), 7.08 (d, J = 8.9 Hz, 1H), 6.56 (s, 1H), 4.28 (t, J = 5.7 Hz, 2H), 3.82 (q, J = 5.5 Hz, 2H), 2.20 (s, 3H), 2.10 (s, 3H). ^{13}C NMR (100 MHz, DMSO-d_6): δ 162.18, 160.37, 159.51, 156.74, 155.57, 155.54, 152.69, 147.64, 143.47, 125.43, 121.68, 115.15, 113.90, 111.19, 110.95, 109.33, 67.19, 40.63, 12.94, 8.45. HRMS (ESI): calcd for $C_{20}H_{16}Cl_3N_4O_3S^+$ (M + H)$^+$, 497.0008; found, 497.0003.

Analytical Data for Compound ***4g***. 7-(2-((5-Chloro-6-(difluoromethyl)pyrimidin-4-yl)amino)ethoxy)-4-(3,4-dichloroisothiazol-5-yl)-8-methyl-2*H*-chromen-2-one, pale yellow solid; yield: 82%; mp 178−179 °C; ^{1}H NMR (400 MHz, DMSO-d_6): δ 8.53 (s, 1H), 8.06 (t, J = 5.7 Hz, 1H), 7.25 (d, J = 8.9 Hz, 1H), 7.08 (d, J = 9.0 Hz, 1H), 7.05 (t, J = 53.1 Hz, 1H), 6.56 (s, 1H), 4.31 (t, J = 5.7 Hz, 2H), 3.90 (q, J = 5.7 Hz, 2H), 2.17 (s, 3H). ^{13}C NMR (100 MHz, DMSO-d_6): δ 160.27, 159.50, 158.98, 156.32, 155.53, 152.68, 152.21 (d, J = 22.9 Hz), 147.65, 143.46, 125.45, 121.69, 115.19, 113.86, 113.11 (d, J = 240.0 Hz), 112.22, 111.00, 109.32, 67.00, 40.63, 8.38. ^{19}F NMR (376 MHz, DMSO-d_6): δ −120.74. HRMS (ESI): calcd for $C_{20}H_{14}Cl_3F_2N_4O_3S^+$ (M + H)$^+$, 532.9820; found, 532.9813.

Analytical Data for Compound ***4h***. 4-(3,4-Dichloroisothiazol-5-yl)-7-(2-((5,6-dichloropyrimidin-4-yl)amino)ethoxy)-8-methyl-2*H*-chromen-2-one, pale yellow solid; yield: 84%; mp

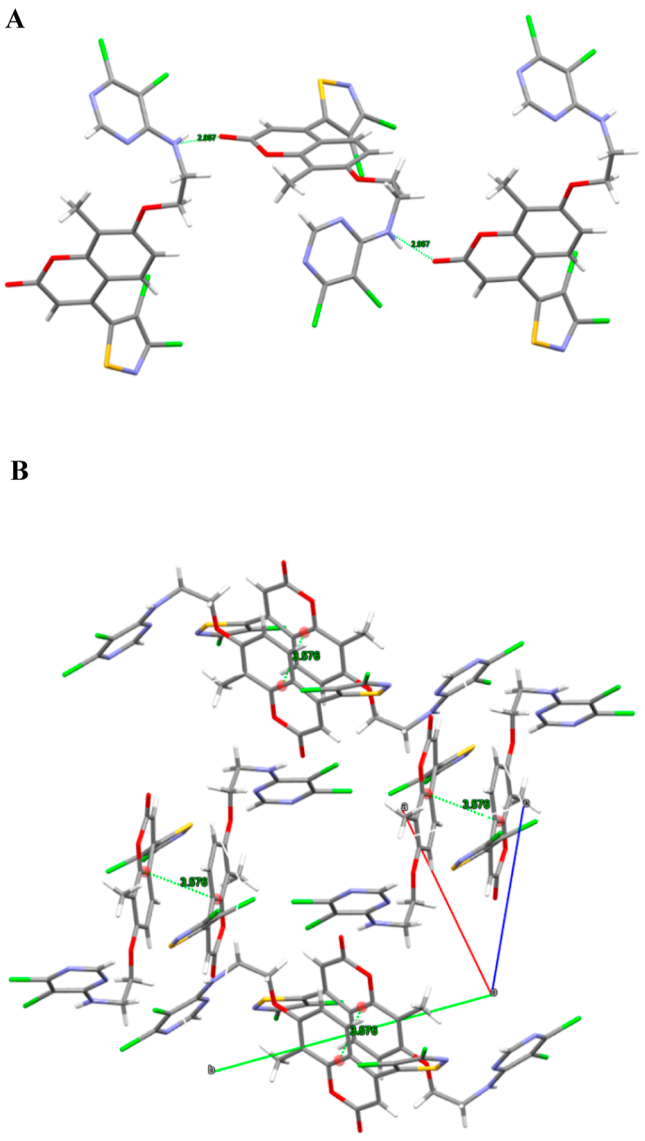

Figure 4. One-dimensional chain structure (A) and stacking structure (B) of **4h**.

203−205 °C; ^{1}H NMR (400 MHz, DMSO-d_6): δ 8.29 (s, 1H), 7.99 (t, J = 5.6 Hz, 1H), 7.24 (d, J = 8.8 Hz, 1H), 7.08 (d, J = 8.9 Hz, 1H), 6.56 (s, 1H), 4.30 (t, J = 5.7 Hz, 2H), 3.87 (q, J = 5.6 Hz, 2H), 2.17 (s, 3H). ^{13}C NMR (100 MHz, DMSO-d_6): δ 160.27, 159.50, 159.44, 155.65, 155.54, 154.97, 152.68, 147.65, 143.46, 125.45, 121.69, 115.19, 113.87, 111.00, 110.41, 109.32, 67.06, 40.69, 8.40. HRMS (ESI): calcd for $C_{19}H_{13}Cl_4N_4O_3S^+$ (M + H)$^+$, 516.9462; found, 516.9460.

Analytical Data for Compound ***4i***. 7-(2-((5-Chloro-6-ethylpyrimidin-4-yl)amino)ethoxy)-4-(3,4-dichloroisothiazol-5-yl)-8-methyl-2*H*-chromen-2-one, white solid; yield: 25%; mp 175−176 °C; ^{1}H NMR (400 MHz, chloroform-*d*): δ 8.44 (d, J = 1.7 Hz, 1H), 7.14 (dd, J = 8.9, 1.6 Hz, 1H), 6.86 (dd, J = 8.9, 1.7 Hz, 1H), 6.33 (d, J = 1.8 Hz, 1H), 5.87 (t, J = 6.1 Hz, 1H), 4.30 (td, J = 5.3, 1.7 Hz, 2H), 4.03 (qd, J = 5.5, 1.7 Hz, 2H), 2.80 (qd, J = 7.6, 1.7 Hz, 2H), 2.37 (d, J = 1.7 Hz, 3H), 1.29−1.24 (m, 3H). ^{13}C NMR (100 MHz, chloroform-*d*): δ 165.22, 160.24, 159.63, 157.62, 155.21, 154.37, 153.01, 149.40, 142.88, 124.48, 122.36, 115.19, 114.95, 112.62, 110.73, 108.18, 67.20, 40.39, 28.08, 11.75, 8.37. HRMS (ESI): calcd for $C_{21}H_{18}Cl_3N_4O_3S^+$ (M + H)$^+$, 511.0165; found, 511.0159.

https://doi.org/10.1021/acsomega.3c05734
ACS Omega 2023, 8, 37471−37481

Table 2. In Vitro Fungicidal Activity of the Compounds at 50 μg/mL[a]

compd.	A. s	B. c	C. a	F. g	P. p	R. s	S. s
2	32 ± 3	42 ± 3	14 ± 3	10 ± 2	0	0	22 ± 2
3	33 ± 1	40 ± 1	33 ± 1	8 ± 1	37 ± 1	65 ± 2	26 ± 3
4a	14 ± 3	63 ± 3	17 ± 1	43 ± 3	15 ± 2	46 ± 2	10 ± 2
4b	17 ± 1	61 ± 3	27 ± 1	41 ± 3	33 ± 3	80 ± 2	20 ± 1
4c	19 ± 3	24 ± 3	18 ± 1	19 ± 3	24 ± 3	55 ± 3	6 ± 1
4d	24 ± 3	36 ± 3	18 ± 1	39 ± 3	10 ± 3	75 ± 2	9 ± 1
4e	0	29 ± 4	11 ± 2	26 ± 3	7 ± 3	49 ± 3	0
4f	36 ± 4	0	21 ± 2	18 ± 1	12 ± 2	48 ± 1	7 ± 1
4g	24 ± 1	64 ± 3	25 ± 1	39 ± 3	9 ± 3	56 ± 1	13 ± 3
4h	17 ± 1	41 ± 2	12 ± 3	25 ± 2	9 ± 1	33 ± 3	0
4i	12 ± 1	25 ± 3	20 ± 1	20 ± 2	0	61 ± 3	12 ± 2
4j	9 ± 2	28 ± 1	20 ± 1	32 ± 4	12 ± 1	62 ± 2	8 ± 2
1[b]	73 ± 2	83 ± 1	79 ± 3	81 ± 1	91 ± 2	83 ± 2	65 ± 1
osthole[b]	14 ± 1	58 ± 1	10 ± 1	17 ± 1	15 ± 1	70 ± 2	33 ± 1
diflumetorim	55 ± 4	44 ± 3	66 ± 2	48 ± 1	39 ± 2	75 ± 1	44 ± 1

[a]A. s, *Alternaria solani*; B. c, *Botrytis cinerea*; C. a, *Cercospora arachidicola*; F. g, *Fusarium graminearum*; P. p, *Physalospora piricola*; R. s, *Rhizoctonia solani*; and S. s, *Sclerotinia sclerotiorum*. [b]Data from ref 26.

Table 3. EC_{50} Value of Target Compounds against *R. solani*

compd.	regression equation	R^2	EC_{50} (μg/mL)	95% confidence interval (μg/mL)
4b	$y = 4.2254 + 0.73450x$	0.9528	11.3	8.61−15.0
4d	$y = 3.4436 + 1.3695x$	0.9874	13.7	11.8−15.9
1[a]	$y = 3.9626 + 1.3553x$	0.9932	5.83	5.31−6.39
osthole[a]	$y = 3.7903 + 1.3147x$	0.9948	8.32	7.59−9.12
diflumetorim	$y = 3.0814 + 1.4806x$	0.9969	19.8	18.1−21.6

[a]Data from ref 26.

Table 4. Binding Affinity of Compounds 4a−4j and Diflumetorim to *Mus musculus* NADH Oxidoreductase

compd.	binding affinity (kcal/mol)	compd.	binding affinity (kcal/mol)
4a	−9.80	**4g**	−10.6
4b	−10.4	**4h**	−10.4
4c	−10.0	**4i**	−10.4
4d	−10.7	**4j**	−10.4
4e	−10.3	diflumetorim	−8.20
4f	−10.5		

Analytical Data for Compound **4j**. 7-(2-((5-Chloro-6-methylpyrimidin-4-yl)amino)ethoxy)-4-(3,4-dichloroisothiazol-5-yl)-8-methyl-2*H*-chromen-2-one, white solid; yield: 44%; mp 201−203 °C; ^{1}H NMR (400 MHz, DMSO-d_6): δ 8.30 (s, 1H), 7.50 (t, J = 5.7 Hz, 1H), 7.24 (d, J = 8.8 Hz, 1H), 7.09 (d, J = 9.0 Hz, 1H), 6.56 (s, 1H), 4.28 (t, J = 5.9 Hz, 2H), 3.84 (q, J = 5.7 Hz, 2H), 2.36 (s, 3H), 2.18 (s, 3H). ^{13}C NMR (100 MHz, DMSO-d_6): δ 160.57, 160.35, 159.52, 158.01, 155.54, 155.30, 152.69, 147.65, 143.48, 125.46, 121.69, 115.15, 113.86, 112.35, 110.97, 109.33, 67.23, 40.62, 21.98, 8.40. HRMS (ESI): calcd for $C_{20}H_{16}Cl_3N_4O_3S^+$ $(M + H)^+$, 497.0008; found, 497.0005.

X-ray Diffraction. The crystal of compound **4h** was cultured using the fusion method and analyzed by X-ray diffraction (Figure 3 and Table 1). The data were collected on a SuperNova single crystal diffractometer equipped with mirror monochromatic Mo Kα radiation (λ = 0.71073 Å) with an ω scan mode at 113.45 K. In the range of $4.142 \leq 2\theta \leq 69.472$, a total of 31,796 reflections were collected, with 7552 unique ones (R_{int} = 0.0482). The structure was solved by direct methods with the XS structure solution program in Olex2 and refined with the ShelXL refinement package by minimizing least squares. Successive difference Fourier syntheses were used to locate all the non-hydrogen atoms. According to the theoretical models, hydrogen atoms were added.

In Vitro Fungicidal Activity. The mycelial growth rate method was used to determine the inhibitory activity of the target compounds against seven plant pathogens, using compound **1**, diflumetorim, and osthole as positive controls. Seven representative fungi, namely, *Alternaria solani*, *Botrytis cinerea*, *Cercospora arachidicola*, *Fusarium graminearum*, *Physalospora piricola*, *R. solani*, and *Sclerotinia sclerotiorum*, were sustainably cultured in our laboratory. Any compounds with inhibitions over 70% were chosen for further median effective concentration (EC_{50}) determination according to reported procedures.[27]

Molecular Docking. Since the crystal structure of complex I NADH oxidoreductase from fungi has not yet been reported. The X-ray crystal structure of the complex I NADH oxidoreductase from *Mus musculus* (pdb: 6ZR2) has been obtained from the Protein Data Bank (https://www.rcsb.org/). ChemDraw 20.1 (PerkinElmer Informatics) was used to draw the structures of the target compounds. Energy minimization was performed using Chem3D 20.1 (PerkinElmer Informatics, Inc.) MM2 energy minimization procedure and saved as a pdb file. Molecular docking procedures were performed using a YASARA (YASARA Biotechnology GmbH). 2D and 3D structures of the complexes were generated by Discovery Studio 2019 (Dassault Systèmes Biovia Corp) and PyMOL (Schrodinger LLC).

Density Functional Theory Calculation. In the study, compounds **4a−4j** were drawn using GaussView 6.0 (Gaussian, Inc.), and their molecular orbital calculations were conducted using Gaussian 09W (Gaussian, Inc.). The structures were

https://doi.org/10.1021/acsomega.3c05734
ACS Omega 2023, 8, 37471−37481

Table 5. Molecular Docking of Compounds 4a−4j to Complex I NADH Oxidoreductase (PDB: 6ZR2)

Compd.	4a	4b	4c	4d	4e
3D diagram	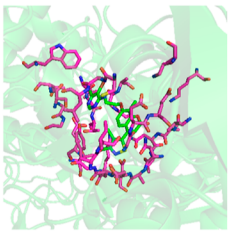	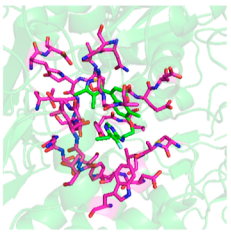	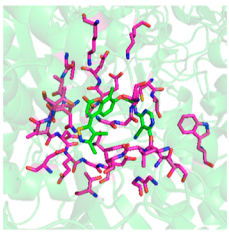	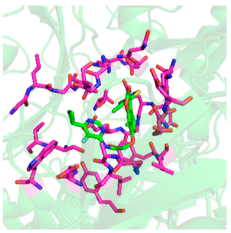	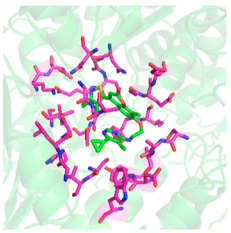
2D diagram	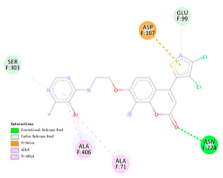	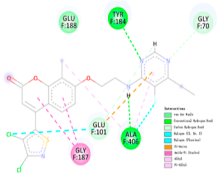	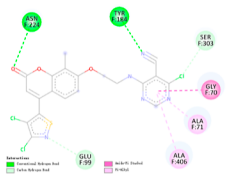	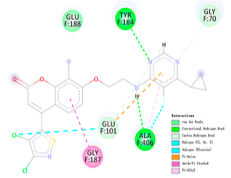	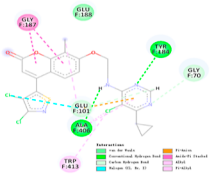
Compd.	4f	4g	4h	4i	4j
3D diagram	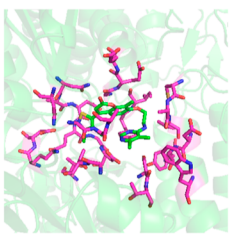	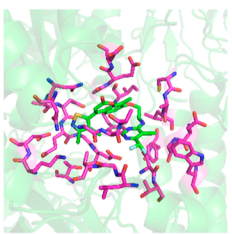	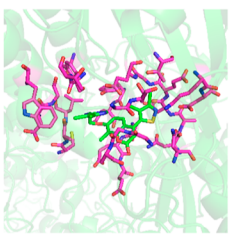	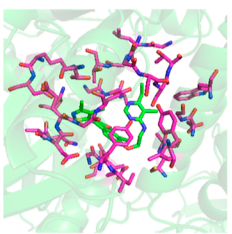	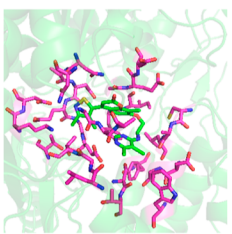
2D diagram	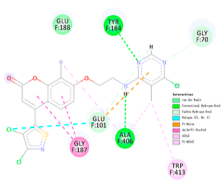	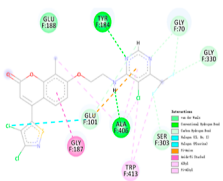	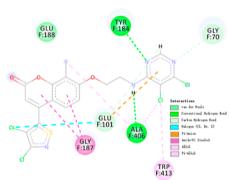	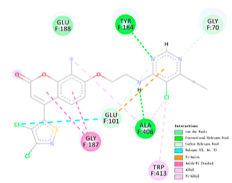	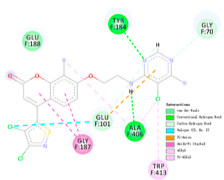

preprocessed and underwent geometric optimization, followed by frequency calculations to ensure geometric stability. The density functional theory (DFT)-B3LYP/6-31G(d) method was employed for these calculations. Subsequently, single-point energy calculations were performed using the DFT-B3LYP/6-31G(d,p) method.

Pesticide Likeness Analysis. To predict the pesticide-likeness properties and bioactivities of the compounds, the SwissADME online tool (http://www.swissadme.ch/) was used for in silico studies. SwissADME is a valuable resource that provides various computational predictions related to pesticide likeness and bioactivity.

RESULTS AND DISCUSSION

Chemicals. Compound **2** was prepared from compound **1** and *tert*-butyl-2-bromoethyl carbamate via nucleophilic substitution under alkaline conditions in 90% yield. Compound **3** was prepared from compound **2** by deprotection of *tert*-butoxy carbonyl with trifluoroacetic acid, and the crude product was used directly in the next reaction without further purification. The target compound **4** was obtained via the nucleophilic substitution reaction of compound **3** and chloropyrimidine under alkaline conditions in 21−87% yields.

Structural Analysis. The bond lengths, bond angles, and torsional angles are shown in Tables S1−S3. All bond lengths and bond angles within the coumarin substructure appear to be normally relative to the closely related compounds in the literature.[14,28] Meanwhile, bond lengths and bond angles within the isothiazole, pyrimidine, and pyranone rings agree well with the values reported.[14] The torsion angle (all close to 180 or 0°) and the measured dihedral angle (0.048°) between the benzene ring and the pyranone ring indicate that the whole coumarin ring is coplanar. Each molecule has a coumarin ring and an isothiazole moiety, with a measured dihedral angle of 55.1° between these two moieties. An intermolecular N−H···O hydrogen bond was observed between the amino group and the carbonyl group on the pyranone ring in the target molecule, with a bond length of 2.96 Å and a bond angle of 152.28°. There is a $\pi-\pi$ interaction between the pyranone rings of two adjacent molecules, with a face-to-center distance of 3.58 Å (Figure 4).

Fungicidal Activity. In vitro fungicidal activity of compounds **4a−4j** at a concentration of 50 μg/mL is presented in Table 2. The target compounds exhibited moderate inhibitory activity against *B. cinerea*, *F. graminearum*, and *R. solani*. Among them, compounds **4a** and **4b** have an inhibitory activity of 63% and 60% against *B. cinerea*, respectively, which is better than the positive controls of osthole and diflumetorim. Compounds **4a**

https://doi.org/10.1021/acsomega.3c05734
ACS Omega 2023, 8, 37471−37481

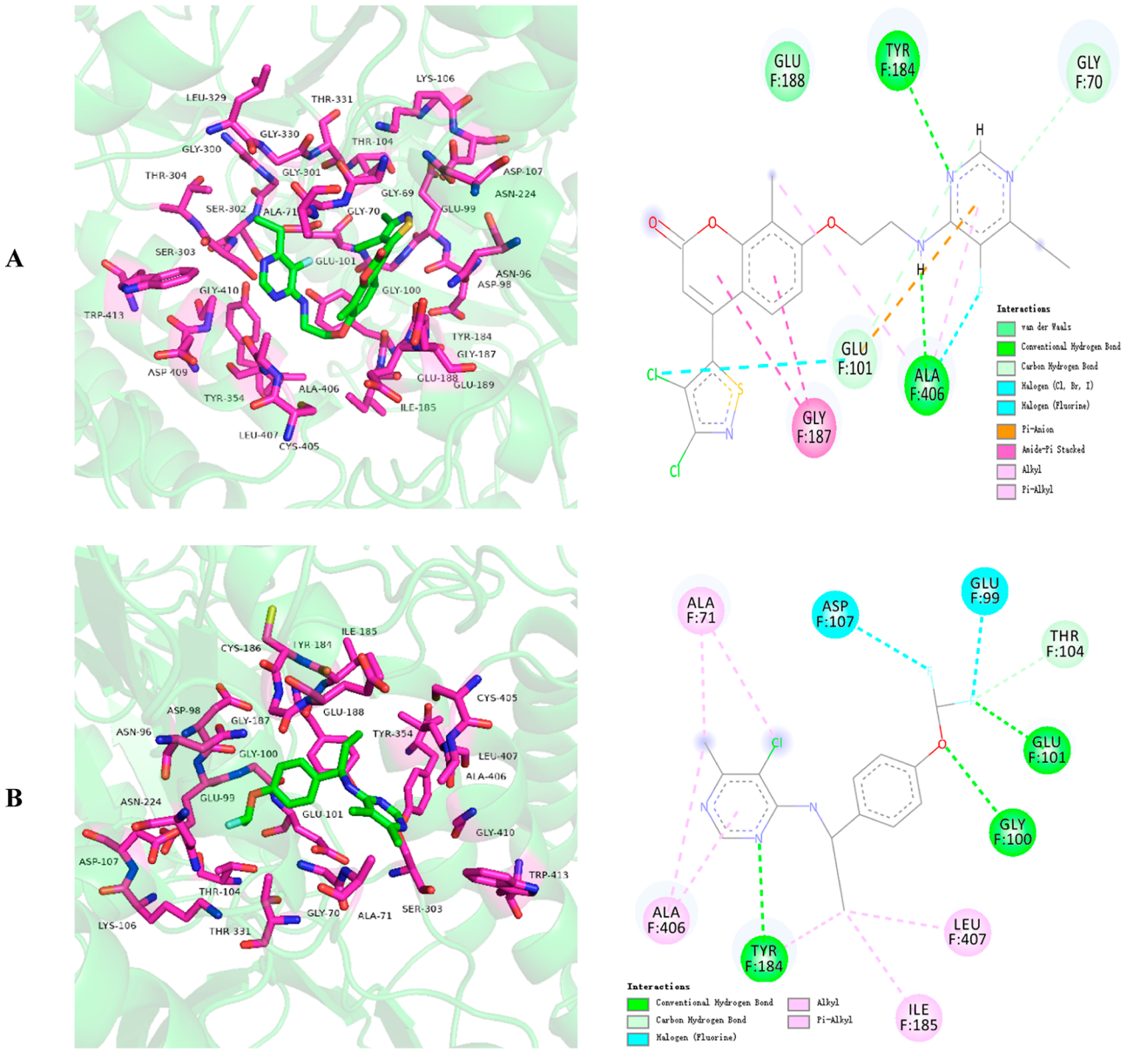

Figure 5. Molecular docking of compound **4b** (**A**) and diflumetorim (**B**) to *Mus musculus* NADH oxidoreductase (pdb: 6ZR2).

Table 6. Low-Energy Conformations of Compounds 4a−4j

Compd.	4a	4b	4c	4d	4e
Conformations	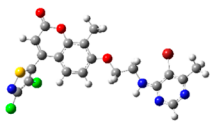	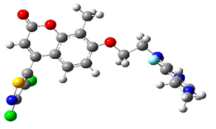	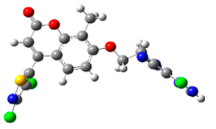	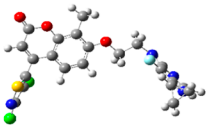	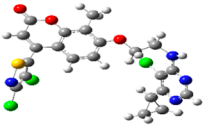
Compd.	**4f**	**4g**	**4h**	**4i**	**4j**
Conformations	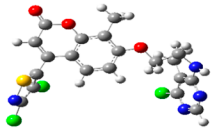	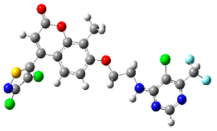	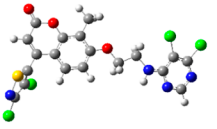		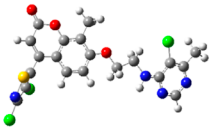

https://doi.org/10.1021/acsomega.3c05734
ACS Omega 2023, 8, 37471−37481

Table 7. HOMO and LUMO of Compounds 4a−4j

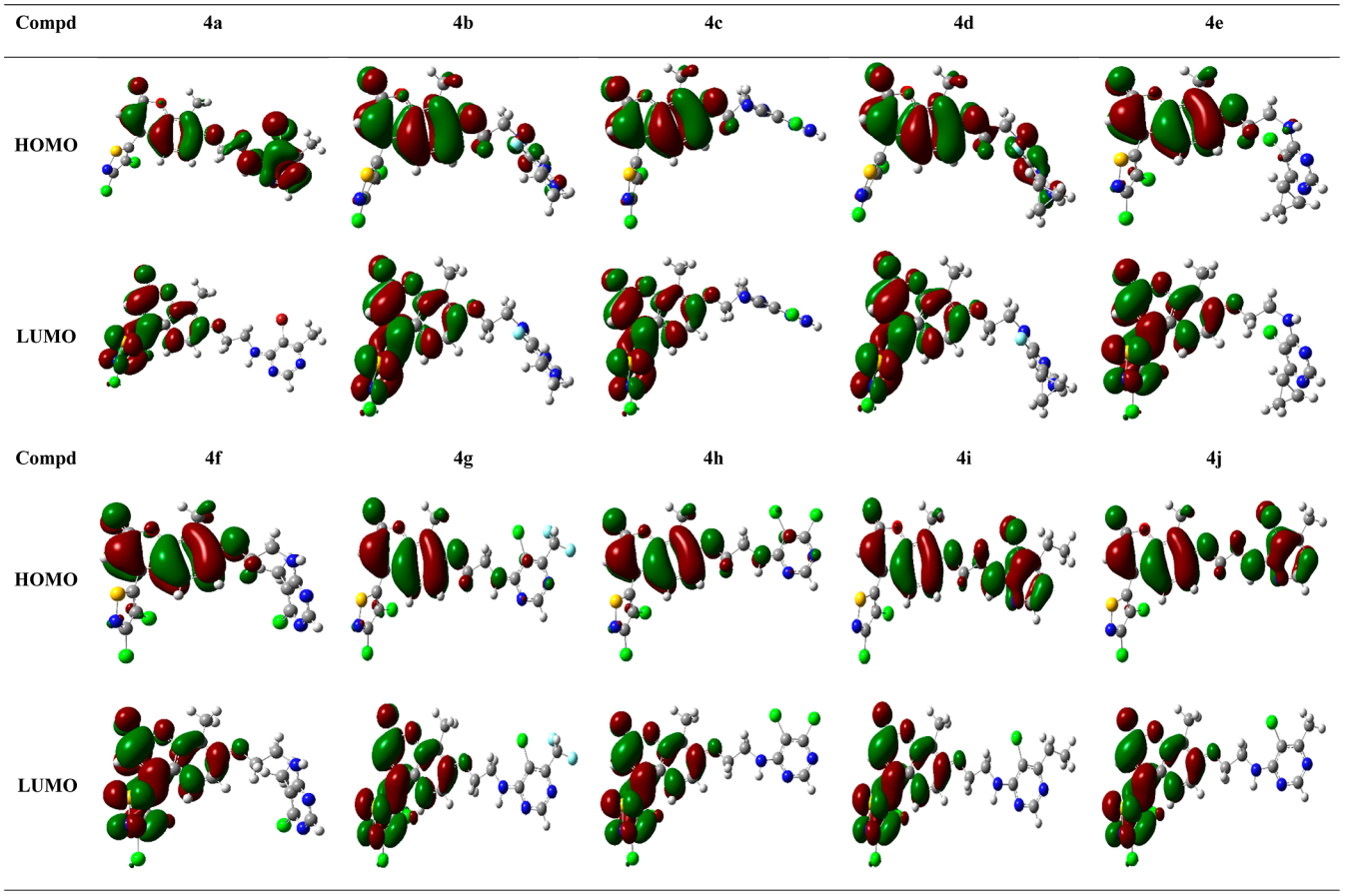

Table 8. FMO Energy of Compounds 4a−4j

compd.	E_{HOMO} (hartree)	E_{LUMO} (hartree)	ΔE (hartree/eV)
1	−0.23646	−0.08930	0.14716/4.00
4a	−0.23678	−0.09097	0.14581/3.97
4b	−0.23549	−0.08888	0.14661/3.99
4c	−0.23551	−0.08807	0.14744/4.01
4d	−0.23497	−0.08857	0.14640/3.98
4e	−0.23498	−0.08850	0.14648/3.99
4f	−0.23839	−0.09065	0.14774/4.02
4g	−0.24113	−0.09290	0.14823/4.03
4h	−0.24111	−0.09286	0.14825/4.03
4i	−0.23704	−0.09082	0.14622/3.98
4j	−0.23748	−0.09087	0.14661/3.99

and **4b** also showed inhibitory activity against *F. graminearum*, superior to that of the positive control osthole. Compound **4b** has 80% inhibitory activity against *R. solani*, which is superior to the positive controls osthole and diflumetorim, and equivalent to the activity of compound **1**. The inhibitory activity of compound **4d** against *R. solani* was 75%, which was superior to the positive control osthole and equivalent to diflumetorim. For *R. solani*, we summarized its structure−activity relationship. The substituent pyrimidine derivatives show fungicidal activity against *R. solani* in the order of **4b** (3-F, 4-CH_2CH_3) > **4d** (3-F, 4-cyclopropyl) > **4j** (3-Cl, 4-CH_3) > **4i** (3-Cl, 4-CH_2CH_3) > **4g** (3-Cl, 4-CHF_2) > **4c** (3-CN, 4-Cl) > **4e** (3-Cl, 4-cyclopropyl) > **4f** (3-CH_3, 4-Cl) > **4a** (3-Br, 4-CH_3) > **4h** (3-Cl, 4-Cl). The activity of the pyrimidine with fluorine at position 3 is higher than that of the pyrimidine with chlorine and bromine in the 3-position. The majority of pyrimidines with chlorine in the 3-position are more active than pyrimidines with other substituents in the 3-position. In summary, fungicidal activity is best when the 3-position contains fluorine, and this provides a direction for further optimization.

To further evaluate the fungicidal activity of the target compounds, the EC_{50} values were determined for the compounds with an inhibition rate greater than 70% at a concentration of 50 μg/mL, as well as lead compound **1**, the positive control osthole, and diflumetorim, and the test results are presented in Table 3. Compounds **4b** and **4d** had good inhibitory activity against *R. solani*, with EC_{50} values of 11.3 and 13.7 μg/mL, respectively, which were better than the positive control diflumetorim (EC_{50} value of 19.8 μg/mL), but inferior to lead compound **1** and osthole.

Molecular Docking Analysis. To validate the mode of action of compounds **4a−4j**, molecular docking was performed (Tables 4 and 5). Also, the docking conformations of compound **4b** and the positive control diflumetorim with complex I NADH oxidoreductase were analyzed (Figure 5). Tyr184 formed hydrogen bonds with both compound **4b** and diflumetorim. Similarly, Ala406 formed an alkyl interaction with the pyrimidine of compound **4b** and diflumetorim. Furthermore, both compound **4b** and diflumetorim form hydrophobic interactions with residues. These results suggest that compound **4b** and diflumetorim may have similar interactions with complex I NADH oxidoreductase.

DFT Calculations. The optimized molecular conformations are listed in Table 6. Molecular total energy, frontier molecular

https://doi.org/10.1021/acsomega.3c05734
ACS Omega 2023, 8, 37471−37481

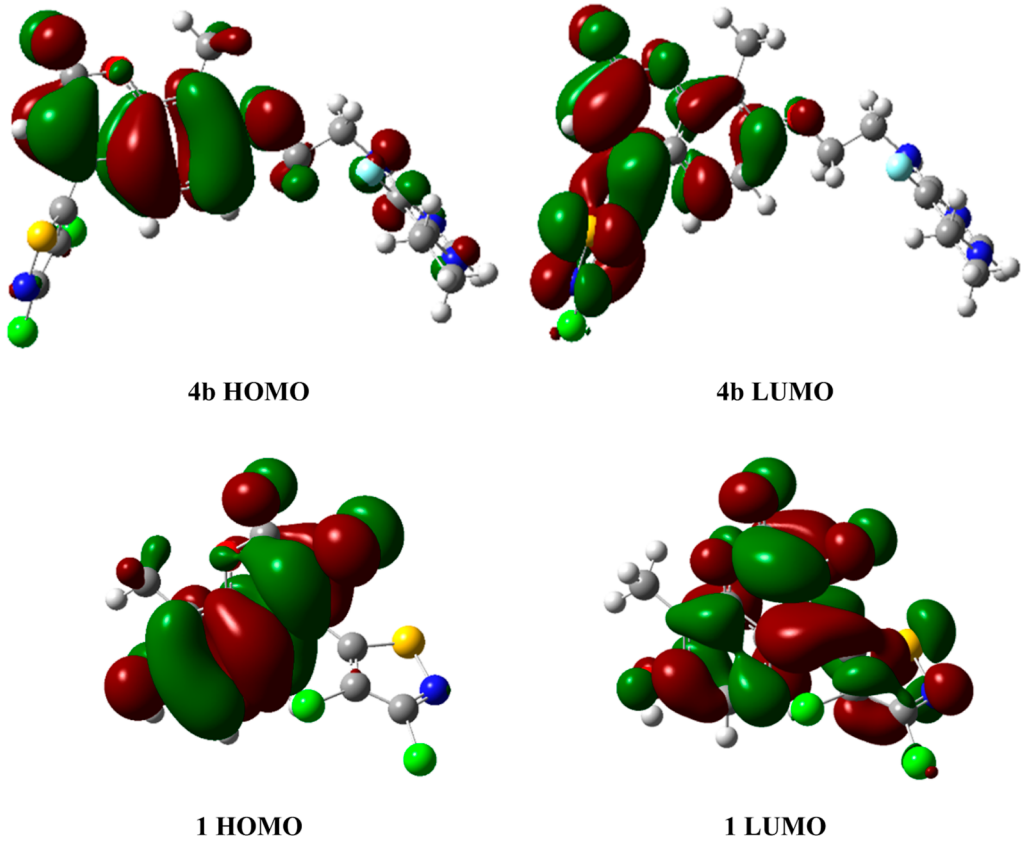

Figure 6. HOMO and LUMO of compounds **4b** and **1**.

Table 9. ADME Properties of Compounds 4a−4j

compd.	M_w	rotatable bonds	H-bond acceptors	H-bond donors	MR (cm^3)	TPSA (Å)	iLOGP	bioavailability score
1	328.17	1	4	1	80.600	91.570	2.58	0.55
4a	542.23	6	6	1	126.96	118.38	4.04	0.55
4b	495.35	7	7	1	124.02	118.38	3.86	0.55
4c	508.76	6	7	1	124.02	142.17	3.51	0.55
4d	507.36	7	7	1	126.72	118.38	4.25	0.55
4e	523.82	7	6	1	131.77	118.38	4.20	0.55
4f	495.81	6	5	1	126.08	97.400	4.47	0.55
4g	533.76	7	8	1	124.37	118.38	3.85	0.55
4h	518.20	6	6	1	124.31	118.38	3.85	0.55
4i	511.81	7	6	1	129.08	118.38	4.18	0.55
4j	497.78	6	6	1	124.27	118.38	3.93	0.55

orbital energy (FMO), and energy gaps between the HOMO and LUMO of compounds **4a−4j** are listed in Tables 7 and 8. The compounds with high activity (**4b**) and positive control **1** were selected for analysis. Their energy gaps between HOMO and LUMO were 3.99 and 4.00 eV, respectively (Table 8).

The LUMO and HOMO influence the electron transition by accepting and donating electrons, respectively, according to FMO theory. In Figure 6, the HOMO of **4b** and **1** was mainly located on the benzopyranone ring, while the LUMO was mainly located on the benzopyranone ring and the isothiazole ring, indicating that the electrons of both compounds were transferred from the benzopyranone ring to the isothiazole ring. This indicates that the direction of electron transfer was the same as that in positive control **1**. The above energy and electron transfer results of **4b** were in approximate agreement with those of **1**, explaining their fungicidal activity on the basis of their chemical structures.

Pesticide-Likeness Analysis. Compounds **4a−4j** were subjected to an ADME study for pesticide-likeness analysis. The pesticide-likeness derived from Lipinski's rule provides a good method.[29,30] It represents the general predictions, such as that the topological polar surface area is not more than 140 Å, the hydrogen acceptor is less than 10 atoms, the hydrogen donor is less than 5 atoms, the molar refractivity is from 40 to 130 cm^3, the octanol−water partition coefficient (log *P*) is between −0.4 and +5.6, and the molecular weight is from 160 to 500 Da. Compounds **4b**, **4f**, and **4j** are pesticide likeness and therefore have the potential to be developed as lead candidates, and the remaining compounds have a molecular weight of just over 500 (Table 9). The MR, TPSA, and iLOGP values of all synthesized compounds **4a−4j** are greater than those of lead compound **1**. We speculate that the increase in MR, TPSA, and iLOGP leads to a decrease in the fungicidal activity of the compounds. In conclusion, the predicted values of the ADME data for

https://doi.org/10.1021/acsomega.3c05734
ACS Omega 2023, 8, 37471−37481

compound **4b** indicate that compound **4b** has the potential to be developed as a lead candidate.

CONCLUSIONS

A series of novel coumarin pyrimidine amine compounds were designed and synthesized. All target compounds were characterized by NMR and HRMS. The bioassay results revealed that compounds **4b** and **4d** display high fungicidal activity against *R. solani*, with EC_{50} values of 11.3 and 13.7 μg/mL, respectively, and both of them were more potent than the positive control diflumetorim. Molecular docking suggested that compound **4b** and diflumetorim may have similar interactions with complex I NADH oxidoreductase. A rational explanation for their fungicidal activity was provided by DFT and pesticide-likeness analysis studies. The results of this study show that compounds **4b** and **4d** deserve further optimization according to the principle of pesticide likeness and provide guidance for the further development of fungicides based on coumarin leads.

ASSOCIATED CONTENT

Supporting Information

The Supporting Information is available free of charge at https://pubs.acs.org/doi/10.1021/acsomega.3c05734.

Single-crystal X-ray data for compound **4h** and ^{1}H NMR, ^{13}C NMR, ^{19}F NMR, and HRMS spectra of target compounds (PDF)

AUTHOR INFORMATION

Corresponding Authors

You Lv − *College of Agricultural and Biological Engineering, Heze University, Heze 274015, P. R. China*; Phone: +86-17302204879; Email: lvyou@hezeu.edu.cn

Zhijin Fan − *State Key Laboratory of Elemento-Organic Chemistry, College of Chemistry, Nankai University, Tianjin 300071, P. R. China; Frontiers Science Center for New Organic Matter, College of Chemistry, Nankai University, Tianjin 300071, P. R. China;* orcid.org/0000-0001-5565-0949; Phone: +86-13920714666; Email: fanzj@nankai.edu.cn; Fax: +86 022-23503620

Authors

Kun Li − *State Key Laboratory of Elemento-Organic Chemistry, College of Chemistry, Nankai University, Tianjin 300071, P. R. China; Frontiers Science Center for New Organic Matter, College of Chemistry, Nankai University, Tianjin 300071, P. R. China;* orcid.org/0009-0003-0039-7167

Mengyuan Li − *State Key Laboratory of Elemento-Organic Chemistry, College of Chemistry, Nankai University, Tianjin 300071, P. R. China; Frontiers Science Center for New Organic Matter, College of Chemistry, Nankai University, Tianjin 300071, P. R. China*

Haolin Zhong − *State Key Laboratory of Elemento-Organic Chemistry, College of Chemistry, Nankai University, Tianjin 300071, P. R. China; Frontiers Science Center for New Organic Matter, College of Chemistry, Nankai University, Tianjin 300071, P. R. China*

Liangfu Tang − *State Key Laboratory of Elemento-Organic Chemistry, College of Chemistry, Nankai University, Tianjin 300071, P. R. China; Frontiers Science Center for New Organic Matter, College of Chemistry, Nankai University, Tianjin 300071, P. R. China*

Complete contact information is available at: https://pubs.acs.org/10.1021/acsomega.3c05734

Notes

The authors declare no competing financial interest.

ACKNOWLEDGMENTS

This work was supported in part by the National Natural Science Foundation of China (no. 32172443); the Science Foundation of Heze University, grant/award no. XY22BS24; and the Frontiers Science Center for New Organic Matter, Nankai University (no. 63181206).

REFERENCES

(1) Li, T.; Lv, M.; Wen, H.; Du, J.; Wang, Z.; Zhang, S.; Xu, H. Natural products in crop protection: thiosemicarbazone derivatives of 3-acetyl-*N*-benzylindoles as antifungal agents and their mechanism of action. *Pest Manage. Sci.* **2023**, *79* (8), 2801−2810.

(2) Tetz, V.; Kardava, K.; Krasnov, K.; Vecherkovskaya, M.; Tetz, G. Antifungal activity of a novel synthetic polymer M451 against phytopathogens. *Front. Microbiol.* **2023**, *14*, 1176428.

(3) Oztekin, S.; Dikmetas, D. N.; Devecioglu, D.; Acar, E. G.; Karbancioglu-Guler, F. Recent insights into the use of antagonistic yeasts for sustainable biomanagement of postharvest pathogenic and mycotoxigenic fungi in fruits with their prevention strategies against mycotoxins. *J. Agric. Food Chem.* **2023**, *71* (26), 9923−9950.

(4) Maimone, N. M.; Junior, M. C. P.; de Oliveira, L. F. P.; Rojas-Villalta, D.; de Lira, S. P.; Barrientos, L.; Nunez-Montero, K. Metabologenomics analysis of pseudomonas sp. So3.2b, an antarctic strain with bioactivity against *Rhizoctonia solani*. *Front. Microbiol.* **2023**, *14*, 1187321.

(5) Obeng, J.; Agyei-Dwarko, D.; Teinor, P.; Danso, I.; Lutuf, H.; Lekete-Lawson, E.; Ablormeti, F. K.; Eddy-Doh, M. A. Bioactivity of an organic farming aid with possible fungistatic properties against some oil palm seedling foliar pathogens. *Sci. Rep.* **2023**, *13* (1), 1280.

(6) Bras, A.; Roy, A.; Heckel, D. G.; Anderson, P.; Karlsson Green, K. Pesticide resistance in arthropods: Ecology matters too. *Ecol. Lett.* **2022**, *25* (8), 1746−1759.

(7) Guan, A. Y.; Liu, C. L.; Li, M.; Zhang, H.; Li, Z. N.; Li, Z. M. Design, synthesis and structure-activity relationship of novel coumarin derivatives. *Pest Manage. Sci.* **2011**, *67* (6), 647−655.

(8) Hao, Z. S.; Wang, W. B.; Yu, B.; Qi, X.; Lv, Y.; Liu, X. Y.; Chen, H. Y.; Kalinina, T. A.; Glukhareva, T. V.; Fan, Z. J. Design, synthesis, and evaluation of fungicidal activity of novel pyrazole-containing strobilurin derivatives. *Chin. J. Chem.* **2021**, *39* (6), 1531−1537.

(9) Gressel, J. Perspective: present pesticide discovery paradigms promote the evolution of resistance - learn from nature and prioritize multi-target site inhibitor design. *Pest Manage. Sci.* **2020**, *76* (2), 421−425.

(10) Sparks, T. C.; Duke, S. O. Structure simplification of natural products as a lead generation approach in agrochemical discovery. *J. Agric. Food Chem.* **2021**, *69* (30), 8324−8346.

(11) Yang, J. L.; Guan, A. Y.; Li, Z. N.; Zhang, P. F.; Liu, C. L. Design, synthesis, and structure-activity relationship of novel spiropyrimidin-amines as fungicides against *Pseudoperonospora cubensis*. *J. Agric. Food Chem.* **2020**, *68* (24), 6485−6492.

(12) Guan, A. Y.; Wang, M. A.; Yang, J. L.; Wang, L. Z.; Xie, Y.; Lan, J.; Liu, C. L. Discovery of a new fungicide candidate through lead optimization of pyrimidinamine derivatives and its activity against cucumber downy mildew. *J. Agric. Food Chem.* **2017**, *65* (49), 10829−10835.

(13) FRAC (Fungicide Resistance Action Committee) Code List*2022, Fungal control agents by cross resistance pattern and mode of action (including coding for FRAC Groups on product labels). www.frac.info (accessed April 21, 2022).

(14) Lv, Y.; Li, K.; Hao, Z.; Kalinina, T. A.; Glukhareva, T. V.; Fan, Z. Synthesis, crystal structure and fungicidal activity of 3-chloro-4-(3,4-dichloroisothiazol-5-yl)5-hydroxy-7-methyl-2*H*-chromen-2-ones. *Chin. J. Struct. Chem.* **2021**, *40* (8), 1068−1074.

(15) Huang, W. Y.; Cai, Y. Z.; Zhang, Y. B. Natural phenolic compounds from medicinal herbs and dietary plants: potential use for cancer prevention. *Nutr. Cancer* **2009**, *62* (1), 1−20.
(16) Chen, L. Z.; Sun, W. W.; Bo, L.; Wang, J. Q.; Xiu, C.; Tang, W. J.; Shi, J. B.; Zhou, H. P.; Liu, X. H. New arylpyrazoline-coumarins: synthesis and anti-inflammatory activity. *Eur. J. Med. Chem.* **2017**, *138*, 170−181.
(17) Hu, Y.; Shen, Y. F.; Wu, X. H.; Tu, X.; Wang, G. X. Synthesis and biological evaluation of coumarin derivatives containing imidazole skeleton as potential antibacterial agents. *Eur. J. Med. Chem.* **2018**, *143*, 958−969.
(18) Thakur, A.; Singla, R.; Jaitak, V. Coumarins as anticancer agents: a review on synthetic strategies, mechanism of action and SAR studies. *Eur. J. Med. Chem.* **2015**, *101*, 476−495.
(19) Foti, M.; Piattelli, M.; Baratta, M. T.; Ruberto, G. Flavonoids, coumarins, and cinnamic acids as antioxidants in a micellar system. Structure-activity relationship. *J. Agric. Food Chem.* **1996**, *44* (2), 497−501.
(20) Liu, Y. P.; Yan, G.; Guo, J. M.; Liu, Y. Y.; Li, Y. J.; Zhao, Y. Y.; Qiang, L.; Fu, Y. H. Prenylated coumarins from the fruits of *manilkara zapota* with potential anti-inflammatory effects and anti-HIV activities. *J. Agric. Food Chem.* **2019**, *67* (43), 11942−11947.
(21) Hassan, M. Z.; Osman, H.; Ali, M. A.; Ahsan, M. J. Therapeutic potential of coumarins as antiviral agents. *Eur. J. Med. Chem.* **2016**, *123*, 236−255.
(22) Zhu, J. J.; Jiang, J. G. Pharmacological and nutritional effects of natural coumarins and their structure-activity relationships. *Mol. Nutr. Food Res.* **2018**, *62* (14), 1701073.
(23) Wang, Q. Q.; Zhang, S. G.; Jiao, J.; Dai, P.; Zhang, W. H. Novel fluorinated 7-hydroxycoumarin derivatives containing an oxime ether moiety: design, synthesis, crystal structure and biological evaluation. *Molecules* **2021**, *26* (2), 372.
(24) Trykowska Konc, J.; Hejchman, E.; Kruszewska, H.; Wolska, I.; Maciejewska, D. Synthesis and pharmacological activity of O-aminoalkyl derivatives of 7-hydroxycoumarin. *Eur. J. Med. Chem.* **2011**, *46* (6), 2252−2263.
(25) Timonen, J. M.; Nieminen, R. M.; Sareila, O.; Goulas, A.; Moilanen, L. J.; Haukka, M.; Vainiotalo, P.; Moilanen, E.; Aulaskari, P. H. Synthesis and anti-inflammatory effects of a series of novel 7-hydroxycoumarin derivatives. *Eur. J. Med. Chem.* **2011**, *46* (9), 3845−3850.
(26) Lv, Y.; Liu, H.; Wang, L.; Li, K.; Gao, W.; Liu, X.; Tang, L.; Kalinina, T. A.; Glukhareva, T. V.; Fan, Z. Discovery of novel 3,4-dichloroisothiazole-containing coumarins as fungicidal leads. *J. Agric. Food Chem.* **2021**, *69* (14), 4253−4262.
(27) Li, K.; Zhang, Y.; Hong, Z. Y.; Yu, Z. W.; Liu, X. Y.; Duan, Z. H.; Gao, W.; Tang, L. F.; Lv, Y.; Fan, Z. J. Design, synthesis and fungicidal activity of ester derivatives of 4-(3, 4-dichloroisothiazole)-7-hydroxy coumarin. *Molecules* **2023**, *28* (13), 5205−5223.
(28) Wang, Z. H.; Li, X. Z.; Wang, L.; Li, P. H. Photoinduced cyclization of alkynoates to coumarins with N-Iodosuccinimide as a free-radical initiator under ambient and metal-free conditions. *Tetrahedron* **2019**, *75* (8), 1044−1051.
(29) Ouyang, Y.; Huang, J. J.; Wang, Y. L.; Zhong, H.; Song, B. A.; Hao, G. F. In silico resources of Drug-Likeness as a mirror: What are we lacking in Pesticide-Likeness? *J. Agric. Food Chem.* **2021**, *69* (37), 10761−10773.
(30) Chen, D. Y.; Hao, G. F.; Song, B. A. Finding the missing property concepts in Pesticide-Likeness. *J. Agric. Food Chem.* **2022**, *70* (33), 10090−10099.

https://doi.org/10.1021/acsomega.3c05734
ACS Omega 2023, 8, 37471−37481